ENTRAINMENT AND MAXIMUM VAPOUR FLOW RATE OF TRAYS

Arnold H. van Sinderen*, E. Frank Wijn and R.W. Jeroen Zanting*****

* Rijks Universiteit Groningen, Department of Chemical Engineering
(Current affiliation: Sulzer Chemtech Ltd, Winterthur, Schw.)
** Meteorenweg 1014, 1443 BD Purmerend, efwijn@euronet.nl
*** Rijks Universiteit Groningen, Department of Chemical Engineering
(Current affiliation: N.V. Nederlandse Gasunie, Groningen, NL)

ABSTRACT

This is a report on free entrainment measurements in a small (0.20 m × 0.20 m) air/water column. An adjustable weir controlled the liquid height on a test tray. Several sieve and valve trays were studied.

The results were interpreted with a two- or three-layer model of the two-phase mixture on the tray. The top or spray layer is gas continuous: in the other layers, the liquid is continuous and contains small bubbles. Large bubbles erupt from the liquid-continuous phase, ejecting drops into the top layer. The distribution of the ejection velocities is taken to be Gaussian. The model allows prediction of the entrainment at different heights and for different gas velocities. As a result, a new equation for the maximum allowable vapour velocity can be presented.

Two regimes were recognized: a 'low-liquid-height' and a 'high-liquid-height' regime. In the low-liquid-height regime, there are only two layers. Here the entrainment *decreases* with increasing liquid height and depends strongly on the type and geometry of the tray deck. At the transition, an intermediate liquid continuous layer develops. In the high-liquid-height regime, there are three layers. Here a further increase in liquid height causes the entrainment to increase. More over the entrainment is independent of the type and geometry of the tray deck.

The results are compared with measurements from F.R.I. on a large tray column. Similar conclusions can be drawn from these measurements, although there are differences due to the difference in scale of the equipment. The model suggests that potentially large gains in the maximum allowable vapour rate of trays should be possible. A way of optimisation of the vapour capacity of existing trays by an appropriate choice of the weir dimensions is presented.

INTRODUCTION

Understanding the hydrodynamic behaviour on trays is of central importance to the design and operation of distillation and absorption columns. Tray hydrodynamics affects pressure drop, liquid height, flow regime, tray efficiency, upper and lower operating limits. A lot of research has gone in their development and improvement. Despite the large amount of experience, we still do not fully understand the behaviour of the gas/liquid mixture on the tray, see Fair, Porter and Zuiderweg in [1, 2]. This paper reports on a multi-layer model of the two-phase mixture. The model was used for interpreting entrainment measurements on sieve and valve trays in a small air/water column [3, 4]. The model will be discussed first.

TRAY MODEL

Structure of the Two-Phase Mixture

Figure 1 shows a tray with a two-phase mixture. Two smaller graphs are included in this figure. The left one shows a typical dispersion density profile; the right one is a probability density curve of the velocity of drops being ejected into the top ('spray') layer.

Three layers are distinguished (of which the middle one is sometimes missing):
- a bottom layer with a high liquid fraction,
- a middle layer with an intermediate (fairly constant) liquid fraction and
- a top layer with a low liquid fraction (gas is the continuous phase).

The height of the bottom layer extends from the tray floor up to H_{btm}. The middle layer extends from H_{btm} to H_o (plane of '**o**rigin of drops') and the top layer from H_o to H_{bed}. Note that the weir height H_W is a separate entity; it does not usually coincide with any of the other heights. The heights of the layers vary with operating conditions and can depend on tray deck geometry. As noted, the middle layer can sometimes disappear.

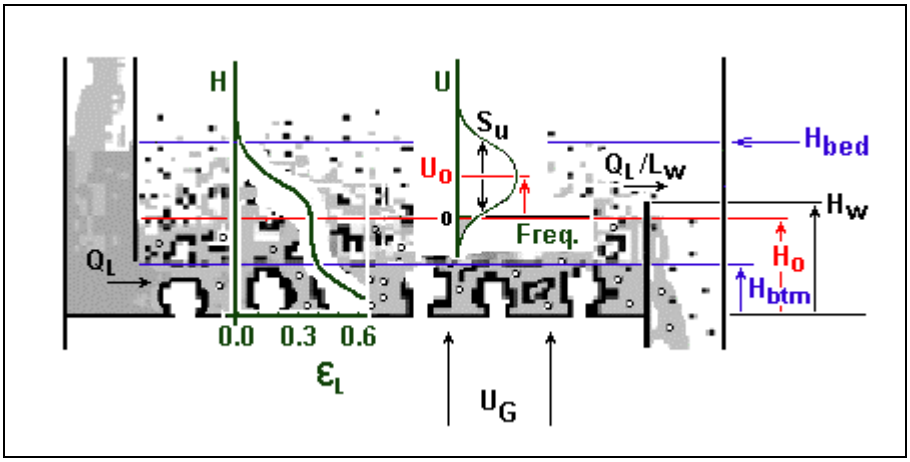

Figure 1. Some concepts and definitions

In the *bottom layer*, bubbles or jets form at the perforations in the tray. The size, shape and pitch of the perforations determine the length scale. These control the size and shape of the bubbles or jets. The time scale is that of the formation of bubbles, or of the pulsation of jets. The characteristic velocity is that of the gas in the holes.

In the *middle layer*, the length scale is that of large bubbles ('voids'). The value is in the range of 0.03..0.06 m. The time scale (about 0.1 s) follows from the eruption frequency of large bubbles. Eruption causes drops to be ejected into the top layer. The velocity scale is that of the rising velocity of the large bubbles (0.3..1 m/s).

The *top layer* consists of drops. One length scale is that of the average drop size. Two others are those of the rise height of the drops (0.05..0.5 m) and their horizontal jumping distance (0.1..0.3 m). The time scale is that of the time of flight of the drops (0.1..0.5 s); the velocity scale that of the ejection velocity of the drops (1..2 m/s).

The Top Layer

The top layer is always a layer of drops. The drops contain a fraction of small bubbles $\varepsilon_{G,s}$. They are ejected from the plane at H_o, with Gaussian velocity distributions, which are 'inherited' from the lower 'liquid'-continuous layer. Figure 1 shows a vertical velocity distribution. The horizontal velocities are randomized uniformly in all directions, see figure 2. The effect of drag on drops will be neglected in the model. This is based on findings from Jeronimo and Sawistowski [5], Hofhuis and Zuiderweg [6] and D.L. Bennett and c.s.[7, 8].

Integrated over a sufficiently large area and long time, the ejected drops generate an upward liquid flux $J_{L,o}$ from the plane at H_o. Considering the full area of this plane to be active, half of it is used for the upward liquid flow and the other half for an equal but downward flow of liquid (assuming a negligible loss by entrainment). The plane at H_o is partly occupied by a 'liquid' phase (with a fraction $\varepsilon_{L,o}$) and partly by large bubbles (with a fraction $1-\varepsilon_{L,o}$). The 'liquid' phase is not a clear liquid but contains a fraction of small bubbles ($1-\varepsilon_{G,s}$). The drops are ejected with an average velocity U_o. This results in an upward clear liquid flux:

$$J_{L,o} = \frac{Q_{L,o}}{A_{ca}} = \frac{1}{2}\left(1-\varepsilon_{G,s}\right)\varepsilon_{L,o}U_o \qquad (1)$$

The liquid height in the top layer, H_L^{top} (assuming no distribution in drop ejection velocity) is given by:

$$H_L^{top} = c_h J_{L,o} t_f \qquad (2)$$

The average time of flight of the drops is: $t_f = 2U_0/g$. The correction factor c_h is introduced to take into account the effect of a distribution in ejection velocity (S_U/U_o). Usually, it falls in the range $1.0 \le c_h \le 1.7$. Combination gives:

$$H_L^{top} = c_h\left(1-\varepsilon_{G,s}\right)\varepsilon_{L,o}\frac{U_o^2}{g} \qquad (3)$$

Erupting Large Bubbles

Already in publications from Davies and Porter [9] and Ashley and Haselden [10] vivid descriptions of the large bubble eruption process can be found. Ejection of drops is caused by successively escaping large bubbles, which erupt with an average frequency ω. A bubble displaces a volume of 'liquid' equal to its own volume. Of this 'liquid' volume, a certain fraction f_{vol} will be ejected from an area given by the cross-section of the bubble. A fraction of the plane of ejection f_{pla} is occupied by large bubbles. Taking into account the small bubble fraction in the 'liquid', the clear liquid flux becomes:

$$J_{L,o} = f_{vol} f_{pla} \left(1 - \varepsilon_{G,s}\right) \left(\frac{6 D_{B,L}^3}{4 D_{B,L}^2} \right) \omega \qquad (4)$$

The large bubble frequency is known to fall in a narrow range of 8..12 s^{-1} [4] and can be approximated by:

$$\omega = 0.71 \sqrt{\frac{g}{D_{B,L}}} \qquad (5)$$

This leads to:

$$J_{L,o} = 1.06 f_{vol} f_{pla} \left(1 - \varepsilon_{G,s}\right) \sqrt{g D_{B,L}} \qquad (6)$$

With $f_{vol} \cong 0.25$, $0.4 < f_{pla} < 0.7$, $0.7 < (1-\varepsilon_{G,s}) < 1.0$, $0.03 < D_{B,L} < 0.05$ m, a rough estimate of the range of the inital liquid flux yields: $0.04 < J_{L,o} < 0.12$ $(m^3/s)/m^2$.

Drop Ejection: The 'Kicking' Mechanism

The envisaged mechanism is one of erupting large bubbles ('voids') and the atomisation of their domes by the gas rushing out accelerating any drops present [11, 12]. The existence of these 'voids' and their importance was first shown by Ashley and Haselden [10]. Bubble rise velocities on sieve trays have been reported by Raper et al. [13]. For large bubbles in the size range from 20 to 80 mm, they found rise velocities in the range of $0.6 < U_{B,L} < 1.2$ m/s. Similar values were found by Ellenberger [14] and de Swart [15] in bubble columns and fluidised beds.

Stichlmair [16] gives a relation for the height of the spray layer on sieve trays. From his equation the contribution of the top layer was extracted and used to calculate the ejection velocity (assuming the fraction of small bubbles $\varepsilon_{G,s}$ was small in his experiments):

$$U_o = 11.2 \frac{\lambda_{ca} \left(1 - \frac{U_B}{U_G}\right)}{1 - \varepsilon_L} \cong 12 \lambda_{ca} \qquad (7)$$

An important consequence of the presence of a substantial concentration of small bubbles in the continuous phase is that the density of the 'liquid' phase becomes less than the density of a clear liquid. The clear liquid density needs to be replaced by the effective 'liquid' density; $(1 - \varepsilon_{G,s})\rho_L$. Thus the ejection velocity is modified as:

$$U_o \cong 12 \frac{\lambda_{ca}}{\sqrt{1 - \varepsilon_{G,s}}} \qquad (8)$$

Liquid Transport by Jumping Drops

Drops in the top not only move up and down, but also horizontally in random directions. The horizontal velocity components will be smaller than the vertical ejection velocity, say $u_{L,hor} = (0.2..0.4)U_o$ or 0.2..0.8 m/s. Drops can jump over horizontal distances of $L_{hor} = u_{L,hor} t_f$ or 0.04..0.32 m. Only droplets generated within a distance of L_{hor} from the weir will jump out and leave the tray.

Consider a point in the middle of the tray, see figure 2 which is reproduced from [17]. In case no preferential direction is imposed on the liquid flow across the tray by the

gas issuing from the perforations and that there is a negligible liquid flow ($u_{L,ca}$) across the tray, the horizontal velocity distribution will be symmetrical. A sufficiently large liquid flow will cause a displacement of this velocity distribution.

Above the weir, the situation is different. No drops come back from the downcomer side, so only the the right half of the velocity distribution remains. It is this half that causes transport of liquid over the weir. The average velocity of the drops flowing over the weir ($u_{L,ow}$) can be equated to the variance of the horizontal velocity distribution ($u_{L,ow} = S_U$). The clear liquid flow rate given by:

$$Q_L = u_{L,ow} L_W H_{L,ow} \tag{9}$$

and the clear liquid height over the weir by:

$$H_{L,ow} = \frac{\left(Q_L / L_W\right)}{u_{L,ow}} \tag{10}$$

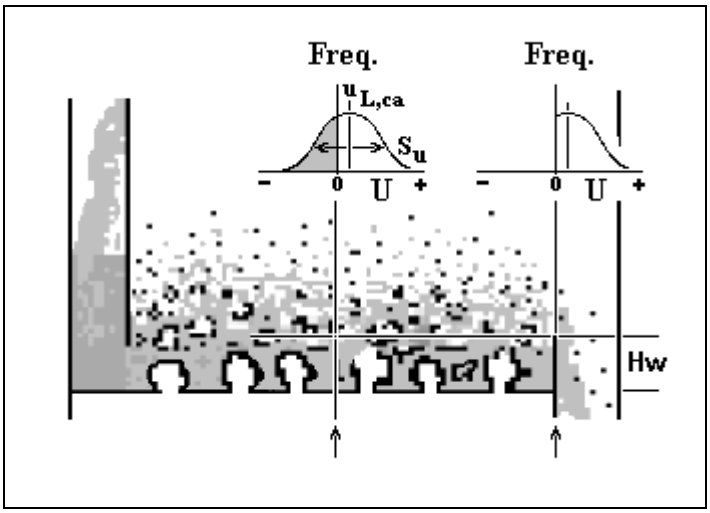

Figure 2. Horizontal velocity distributions

This mechanism only applies when the drops jumping around in the top layer can supply the same (or a larger) flow rate than the liquid flow rate supplied to the tray; $Q_L^{top} \geq Q_L$. For this to work, sufficient liquid has to be kept 'in flight' in order to be transported. So, the liquid hold up in drops 'in flight' has to provide the required 'weir crest'; $H_L^{top} \geq H_{L,ow}$ .When this condition is fulfilled, the weir is above the drop ejection plane H_o. Then the position of the plane can be found from:

$$H_L^{top} = H_{L,ow} + \varepsilon_{L,o}\left(H_W - H_o\right) \tag{11}$$

By rearrangement and substitution of equations (3) and (10):

$$H_o = H_W - c_h\left(1 - \varepsilon_{G,s}\right)\frac{U_o^2}{g} + \frac{\left(Q_L / L_W\right)}{\varepsilon_{L,o} u_{L,ow}} \tag{12}$$

This is an important equation. It shows that the drop ejection plane will move freely in response to changes in the operating conditions, tray layout and system properties. However, this mobility reaches a limit, when the ejection plane moves on top of the bottom layer; $H_o = H_{btm}$. When this happens, the bubble formation and/or jet-formation processes at the perforations in the tray floor are expected to come into play and the model needs to be modified.

From Three to Two Layers: A New Transition

The *middle layer* extends up from H_{btm} to H_o. The drop ejection plane can move up or down by adjustment of the weir height. When the weir height is moved down far enough H_o will be on top of the bottom layer; $H_o = H_{btm}$ and the middle layer will have disappeared. At this transition point there are only two contributions to the liquid height, one from the top layer and another from the bottom layer. At liquid heights below the transition liquid height ($H_{L,tr}$) a two-layered two-phase mixture exists. The transition liquid height is just the amount of liquid needed to submerge and saturate the bottom layer and at the same time maintain the top layer at the prevailing conditions:

$$H_{L,tr} = H_L^{btm} + H_L^{top} = \left(1-\varepsilon_{G,s}\right)\varepsilon_{L,o}H_{btm} + c_h\left(1-\varepsilon_{G,s}\right)\varepsilon_{L,o}\frac{U_o^2}{g} \qquad (13)$$

Addition of any liquid in excess of this will go into the formation of a middle layer. In this case, the large bubbles get the chance to grow further. The 'liquid'-continuous phase will continually be overturned and mixed by random motions associated with coalescence and rise of the large bubbles. This process decouples the behaviour in the upper layers from the behaviour in the bottom layer.

Bed and Liquid Height

The height of the two-phase mixture is the sum of two contributions: the height of the lower 'liquid'-continuous layers and the height of the top layer. The height occupied by the top layer is defined by an arbitrarily chosen, but consistently used point on the high tail of the projection velocity distribution with velocity ($U_o + kS_U$):

$$H_{bed} = H_o + \frac{\left(U_o + kS_U\right)^2}{2g} = H_o + \left(1+\frac{kS_U}{U_o}\right)^2\frac{U_o^2}{2g} \qquad (14)$$

In the following, a correction factor c_{SU} will be introduced; $c_{SU}= (1+(kS_U/U_o))^2$. This correction factor accounts for drops having an ejection velocity larger than the average value U_o.

For the two-layered mixture (with H_o = H_{btm} and H_{btm} being tray specific), this becomes simply:

$$H_{bed} = H_{btm} + c_{SU}\frac{U_o{}^2}{2g} \qquad (15)$$

For the three-layered mixture (with $H_o > H_{btm}$ and H_o free to move in response to changes in operation conditions, etc.), equation (12) is used to obtain:

$$H_{bed} = H_W + \left(c_{SU} - 2c_h(1-\varepsilon_{G,s})\right)\frac{U_o{}^2}{2g} + \frac{\left(Q_L/L_W\right)}{\varepsilon_{L,o}u_{L,ow}} \qquad (16)$$

Similarly, the clear liquid height can be obtained by summation of the contributions of the 'liquid'-continuous layers and the top layer:

$$H_L = \left(1-\varepsilon_{G,s}\right)\varepsilon_{L,o}H_o + H_L^{top} \qquad (17)$$

For a two-layered mixture:

$$H_L = \left(1-\varepsilon_{G,s}\right)\varepsilon_{L,o}H_{btm} + c_h\left(1-\varepsilon_{G,s}\right)\varepsilon_{L,o}\frac{U_o^2}{g} \qquad (18)$$

For the three-layered mixture:

$$H_L = \left(1-\varepsilon_{G,s}\right)\varepsilon_{L,o}H_W + c_h\varepsilon_{G,s}\left(1-\varepsilon_{G,s}\right)\varepsilon_{L,o}\frac{U_o^2}{g} + \left(1-\varepsilon_{G,s}\right)\frac{\left(Q_L/L_W\right)}{u_{L,ow}} \qquad (19)$$

Entrainment and Maximum Allowable Vapour Flow Rate

The initial droplet flux generated at height H_o is: $J_o = Q_o/A_{ca}$. The free drop entrainment flux collectable at height H_E , $J_E = Q_E/A_{ca}$ will be only a fraction f_E of the initial droplet flux:

$$J_E = f_E J_o \qquad (20)$$

This fraction can be evaluated from the drop ejection velocity distribution.

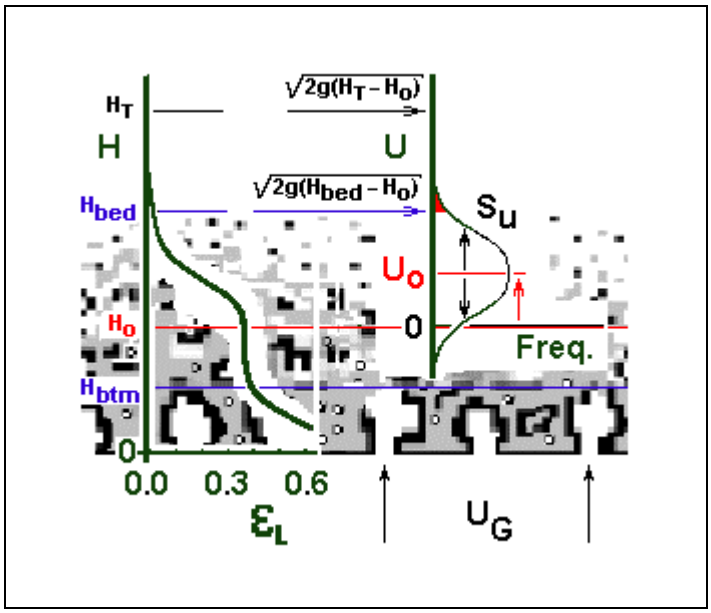

Figure 3. Drop ejection velocity distribution

The ejection velocity distribution is characterized by the average velocity U_o; the standard deviation in velocity S_U; and the velocity 'threshold' $\sqrt{(2g(H_E - H_o)}$ to reach the entrainment collection height H_E). A drop with initial velocity U will scale a difference in height $(H - H_o) = U^2/2g$ (drag by the gas is being neglected). By integration of the high-end tail of the Gaussian velocity distribution, the entrainment fraction can be evaluated:

$$f_E = \int_{\sqrt{2g(H_E-H_o)}}^{\infty} \mathbf{P}\left(\sqrt{2g\left(H_E-H_o\right)};U_o;S_U\right)\mathrm{d}U \qquad (21)$$

using: $$\mathbf{P}\left(\sqrt{2g\left(H_E-H_o\right)};U_o;S_U\right) = \frac{1}{\sqrt{2\pi}}e^{\left(-\frac{Z^2}{2}\right)} \qquad (22)$$

with: $$Z = \frac{\sqrt{2g\left(H_E-H_o\right)}-U_o}{S_U}$$

Then, the entrainment fraction is obtained from the complement of the error function:

$$f_E = 1 - \mathbf{erf}(Z) \tag{23}$$

During the evaluation of the experimental data, a simple exponential function was used as an approximation to equation 23, at sufficiently large values of Z (> 1.5). This approximation holds over a range of f_E-values of two or more decades, with a remarkable 'goodness of fit' ($0.99 < R^2 < 1$):

$$f_E = Ae^{-Bz} \tag{24}$$

By combining equations (20) and (24), the following approximating relation is obtained:

$$J_E = AJ_o e^{-B\frac{\sqrt{2g(H_T - H_o)} - U_o}{S_U}} \tag{25}$$

For certain conditions, the entrainment collected by a next higher tray (in a set of trays) can set a limit to the *maximum allowable gas flow rate*. The collected entrainment will be directly dependent on the free entrainment rate from the tray below, as well as on the entrainment collection efficiency of the tray. At present, preciously little is known about the entrainment collection efficiency of trays, therefore it will be assumed that the fraction of free open area of the tray governs the collection efficiency: $J_{E,c} = f_h J_E$. It will be assumed that the ratio $(J_{E,c}/J_o)_{max}$ will exceed an arbitrary maximum value at the occurrence of the *maximum allowable gas flow rate*.

To find this *maximum allowable gas velocity*, equation (24) is rewritten by making the Z-value explicit. This gives a relationship between tray spacing H_T, maximum drop velocity $U_{o,max}$, standard deviation of the drop velocity distribution S_U and a conveniently chosen entrainment criterion:

$$\frac{\sqrt{2g\left(H_T - H_o\right)} - U_{o,max}}{S_U} = \frac{ln\left(f_h\right) + ln\left(A\right) - ln\left(J_{E,c}/J_o\right)_{max}}{B} = c_{max} \tag{26}$$

Then, the maximum allowable drop ejection velocity can be represented by:

$$U_{o,max} = \sqrt{2g\left(H_T - H_o\right)} - c_{max} S_U \tag{27}$$

This remarkably relation has important practical consequences. The first of these can be shown by introducing equation (8) for the ejection velocity. This gives for the *maximum allowable gas velocity*:

$$\lambda_{ca,max} = \frac{\sqrt{1 - \varepsilon_{G,s}}}{12}\sqrt{2g\left(H_T - H_o\right)} - c_{max}\frac{\sqrt{1 - \varepsilon_{G,s}}}{12} S_U \tag{28}$$

The familiar approximate square root dependence of the maximum load factor λ_{ca} on tray spacing is reproduced. Secondly, the square root term $\sqrt{(1-\varepsilon_{G,s})}$ now takes on the special meaning of a *'de-rating factor'*, also known as *'system factor'* or *'foam factor'*. Thirdly, it introduces the concept of a *minimum tray spacing* needed to accommodate the high-end tail of the fluctuations in the ejection velocity. Stated otherwise, a minimum 'freeboard' height is required to cater for the 'restlessness' in the two-phase mixture. To achieve operability of a tray, $\lambda_{ca,max} \geq 0$, thus:

$$H_{T,min} = H_o + \frac{c_{max}^2 S_U^2}{2g} \tag{29}$$

Equation (29) can be compared with an equation derived from the bed height equation (14). Recognizing that the maximum dispersion height is constrained by the tray spacing $H_T = H_o + (U_{o,max} + kS_U)^2/2g$ and using equation (8):

$$\lambda_{ca,max} = \frac{\sqrt{1-\varepsilon_{G,s}}}{12}\sqrt{2g(H_T - H_o)} - k\frac{\sqrt{1-\varepsilon_{G,s}}}{12}S_U \tag{30}$$

This shows that the maximum gas rates for the entrainment limitation and for the bed expansion limitation are quite similar. What remains is only a small *difference in maximum gas rate* ($\Delta\lambda_{ca,max}$) between the maximum gas rates derived from equations (28) and (30):

$$\Delta\lambda_{ca,max} = \left(\frac{c_{max} - k}{12}\right)S_U \tag{31}$$

This difference in maximum capacity depends only on the spread in the ejection velocity distribution S_U and on the criteria implied by the use of the constants c_{max} and k.

EXPERIMENTAL

The Test Rig

A small-scale (0.2 m $\times$ 0.2 m) test unit for the study of two-phase flow behaviour on contacting trays was built at the Chemical Engineering Department of the University of Groningen. The aim of the test unit and test programme was to provide test data on the mass transfer behaviour and on the dynamic behaviour of the gas and liquid phases flowing across a single contacting tray. Detailed information on the test unit, test programme, techniques and the data obtained with this unit has been collected in the "Groningen Tray Test Rig, Data Report", December 2000 [3].

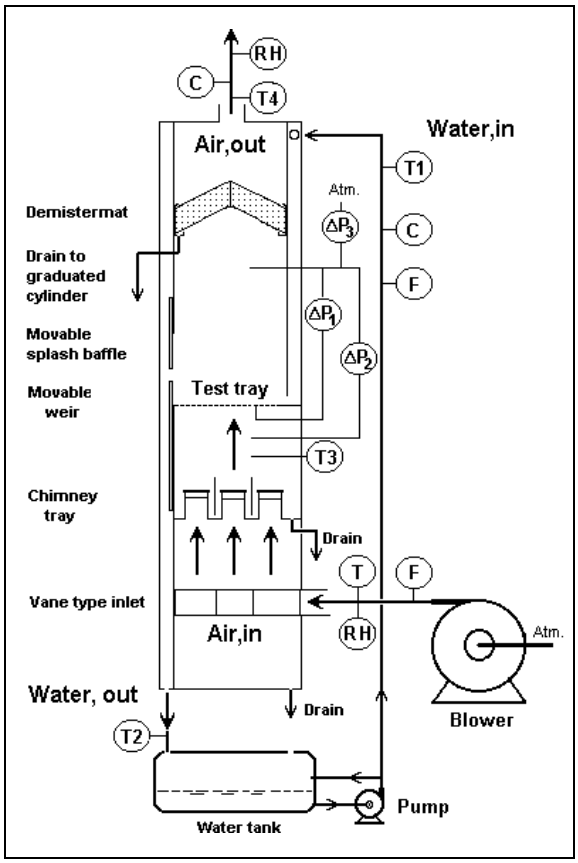

Figure 4. Schematic of Test Rig

The Groningen Tray Test Rig had a special combination of characteristics defining its capabilities:

- an exchangeable tray floor;
- an outlet weir, which is continuously variable in height, during operation;
- a splash-baffle above weir, also continuously variable in height, during operation;
- measurement of entrained droplets by a mesh pad, which can be drained and can be set at any desired height (above the outlet weir), during operation;
- measurement of weeping rate of liquid, by collection on the lower chimney tray;
- fast responding transducers for pressure drop measurements;
- adjustable air- and water flow rates.

In setting up our test unit, the favourable experience of R. Thorogood and R. Sacks, the pioneers of this type of approach [18], was used as guidance.

Entrainment Measurement

The demister pad (mesh pad) used to collect the entrained droplets can be varied in height from essentially the tray floor to the top of the column. The heigt of the demister pad is measured from the tray floor to the underside of the rectangular water discharge gutter (below the mesh pad). By adding the height of the gutter (0.025 m) and a height difference (of 0.022 m) the mean horizontal mesh pad position was obtained. The inlet area of the mesh pad (0.166 $\times$ 0.174 m) is 72.2% of the contacting area of the test tray underneath. The reported entrainment flux is defined as measured flow rate divided by mesh pad inlet area; Q_E/A_{mat}. The liquid discharging from the gutter is collected in a measuring cylinder. The maximum water discharge capacity was 48 $\times$ 10^{-3} m^3/h, which limited the entrainment measurement to 4.8% of the maximum water flow rate (of 1 m^3/h). Entrainment rates exceeding this value led to an overflowing gutter. Hence, the maximum measurable entrainment flux was limited to values below Q_E/A_{mat}= 4.5 $\times$ 10^{-4} (m^3/s)/m^2.

Trays tested

The focus of this paper is on the dynamic behaviour of the gas/liquid layer on a tray. Obviously, the way of injecting gas into this layer plays a central role. To elucidate the eventual similarities and differences in the performance characteristics, three different types of tray were studied:

- **sieve trays** with 6 mm diameter and with 12 mm diameter holes (vertical upward gas injection, without a preferred direction in the horizontal plane);

- trays with **fixed-valves** (Nutter MVG and Nutter μVG)

(horizontally sideways gas injection through two fixed trapezoidal slots per valve and to a small
extent directed to the outlet weir);

- trays with **moving-valves**,
either round valves (Snap-In valves of Shell and Sulzer Chemtech)
or rectangular valves (Nutter BDH valves)
(peripheral horizontal sideways gas injection through two variable rectangular slots per valve,
without preferred direction either forward or backward)

The trays were made of stainless steel sheet material, 2 mm thick. All plates were square 0.200 m × 0.200 m. The square shape of the contacting area enabled trays, with an asymmetric perforation pattern or with horizontally directed gas injection, to be rotated by 90° or 180°. Thus, the effect of directional gas injection into the two-phase layer could be studied.

Table 1. Summary of trays tested

Tray Code	Type	N #	Pitch pattern	Pitch mm×mm	D_h mm	FA %
ST 85	Sieve plate	85	Δ	17.5×17.5	6	6.0
ST 27	Sieve plate	27	Δ	41.3×43.7	12	7.6
MVG	mini V-Grid	13	Δ	58×76		14.8
μVG	micro V-Grid	36	Δ	38×51		20.0
KS 4	Snap-In valve (round)	6	□	100×100	40	12.6
KS 6	Snap-In valve (round)	6	□	60×100	40	18.9
BDH 375	Rectangular valve	8	□	54×79		25.4

Note: The Free Area (FA) of the sieve trays, the round valves and the rectangular valves is based on the fixed open area in the tray floor and related to the contacting area. For the MVG and μVG fixed-valve trays, the Free Area is based on the vertical (curtain) area of the side slots.

Air and water (at ambient conditions) were used as test system. In this paper, almost all reported data were obtained with R.O. (reverse osmosis) water.

The test programme included studying liquid entrainment, liquid leakage, tray pressure drop and static liquid height and their fluctuations could be recorded simultaneously, at the same operating condition. In an unconventional way, the liquid height was varied systematically by changing the weir height; at certain fixed air flow rates, for the seven tray decks studied.

Most of the test runs were run at one fixed water flow rate (Q_L = 1.0 m^3/h) and three different
fixed air flow rates, see table 2 and 3.

Table 2. Standard water flow rate

Q_L m^3/h	Q_L / A_{ca} m/s	Q_L / L_W $(m^3/s)/m$
1.00	0.0069	0.0014

Table 3. Standard air flow rates and velocities in the contacting area

Q_g m^3/h	F-factor, F_{ca} $m/s\sqrt{(kg/m^3)}$	Load factor, λ_{ca} m/s
150	1.23	0.039
225	1.86	0.059
300	2.46	0.078

EXPERIMENTAL RESULTS and DISCUSSION

Example: the MVG Tray

For the three standard gas flow rates, a graph of entrainment rate versus liquid height (figure 5) shows two distinct ranges in the entrainment behaviour separated by a shallow minimum. Below a liquid height in the range from about 0.03 to 0.04 m, the entrainment rate is hardly affected by an increase in liquid height (at the lowest gas rate) or decreases with an increasing liquid height (two highest gas rates). In the transition range, there is either a '*break'* in the curve (for the lowest gas rate) or a *minimum* in the entrainment rate (for the two highest gas rates). Above the transition range, the entrainment rate increases monotonously. The drawn curves represent the behaviour of equation (32) for each of the three gas flow rates. At higher gas rates, less liquid is needed to generate the same change in dispersion height, because of a lower dispersion density. This explains the increase in slope of the drawn curves. Also, this emphasises that it is the underlying change in weir height (which caused the increase in liquid height) that governs the entrainment rate, because it controls the level of the plane of origin of the drops (equation 12). Earlier references to the effect of a change in weir height causing a minimum in entrainment rate have (not yet) been found in the literature. However, there do exist references showing that a change in weir load can cause a minimum in the entrainment rate [20-22]. Note, that the effect of weir load is taken into account by equation (12), as well.

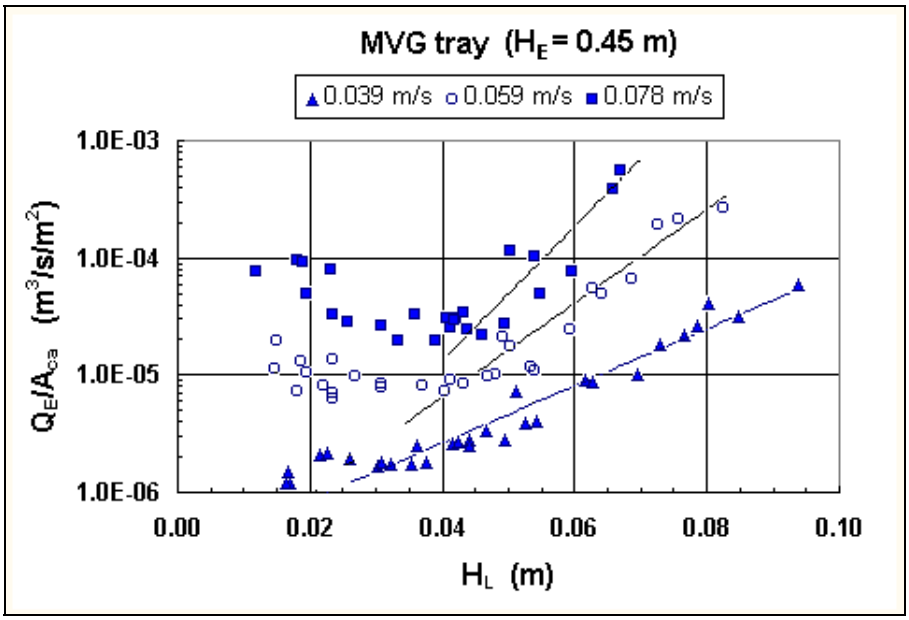

Figure 5. Entrainment rate for MVG tray, at H_E = 0.45 m.

In the further analysis, the data will be divided in two parts. The first part deals with the 'low-liquid- height' regime and the second part with the 'high-liquid-height' regime. In the 'low-liquid-height' regime the entrainment rate at the two weir heights of 0.000 m and 0.050 m will be examined to show its sensitivity to several parameters. For the second part of the entrainment data their interpretation is based on equation (25), which suggested a linear dependence between $\ln(Q_E/A_{ca})$ and a group (being part of the earlier mentioned z-value and) contains the important variables, viz. $\{\sqrt{[2g(H_E - H_o)]} - U_o\}$. In using this group, note that equation (8) is used for the ejection velocity. Clearly, attention has to be paid to the effect of the position of the plane of origin of the ejected droplets, H_o, which is expected to move up and down along with the weir height H_W according to equation (12).

The 'Low-Liquid-Height' Regime

Table 3 illustrates the entrainment behaviour in the 'low-liquid-height' range for two fixed weir heights (0.000 and 0.050 m). Apart from a dependence on weir height (or liquid height), the entrainment rate depends sensitively on gas rate and position of the entrainment collector (mesh pad) above the tray.

Table 3. MVG tray operating at low liquid heights

MVG		**H_E = 0.25 m**		**H_E = 0.35 m**		**H_E = 0.45 m**	
	Weir height (m)	**Q_E/A_{mat} (m/s)**	**Q_E - ratio**	**Q_E/A_{mat} (m/s)**	**Q_E - ratio**	**Q_E/A_{mat} (m/s)**	**Q_E - ratio**
λ_{ca} = 0.039 m/s	0.000	2.4×10^{-5}	**0.58**	4.0×10^{-6}	**0.47**	1.2×10^{-6}	**0.72**
	0.050	4.2×10^{-5}	1.00	8.5×10^{-6}	1.00	1.7×10^{-6}	1.00
λ_{ca} = 0.059 m/s	0.000	2.3×10^{-4}	**1.53**	6.2×10^{-5}	**2.38**	1.9×10^{-5}	**2.30**
	0.050	1.5×10^{-4}	1.00	2.6×10^{-5}	1.00	8.4×10^{-6}	1.00
λ_{ca} = 0.078 m/s	0.000	7.3×10^{-4}	**1.46**	1.9×10^{-4}	**1.43**	9.6×10^{-5}	**1.78**
	0.050	5.0×10^{-4}	1.00	1.4×10^{-4}	1.00	5.4×10^{-5}	1.00

The 'High-Liquid-Height' Regime

The test range for the weir height was $0.025 \leq H_W \leq 0.300$ m and for the height of the entrainment collector was $0.250 \leq H_E \leq 0.450$ m. Data for test conditions with large amplitude waves in the height of the dispersion ('oscillations') have been excluded.

Table 4. MVG tray operating at high liquid heights

λ_{ca} (m/s)	$H_W \geq$ (m)	$Q_E/A_{mat} = a \exp^{b(HE-cHw)}$ a	b	c	R^2 (–)
0.039	0.025	2.2×10^{-3}	-18.30	0.75	0.971
0.059	0.050	7.2×10^{-3}	-19.38	0.70	0.967
0.078	0.100	16.7×10^{-3}	-18.52	0.55	0.969

Table 4 shows that an exponential relation gives a good representation ($R^2 > 0.95$) of the entrainment behaviour over a large range of variation in entrainment flux Q_E/A_{mat} (1 to 2 decades). Notice that for the exponential relation to be applicable, the weir height is required to be above the indicated approximate threshold values. The pre-exponential coefficient *a* increases strongly with an increase in gas flow rate λ_{ca}. The exponent *b* varies within a very small range and may be treated as a constant; $b = -18.5 \pm 0.5$. The exponent *c*, correcting the effect of weir height, may be considered constant at a specific gas flow rate. Its value decreases with an increase in gas flow rate (at $\lambda_{ca} = 0.039$ m/s, $c = 0.73 \pm 0.03$; at $\lambda_{ca} = 0.059$ m/s, $c = 0.71 \pm 0.03$; at $\lambda_{ca} = 0.078$ m/s, $c = 0.57 \pm 0.02$). This indicates that the effect of an increasing liquid hold up in the top ('spray') layer, which at the same time lowers the plane of origin of the drops H_o. This effect needs to be taken into account.

From these results, it was derived that an increase in distance of the tray to the mesh pad by about 0.050 m halves the entrainment rate. An increase in weir height by about 0.050 to 0.075 m doubles the entrainment rate. An increase in gas rate of some 25 to 30 % increases the entrainment rate by a factor two. This emphasizes the sensitivity to changes in height of measurement, weir height and gas flow rate.

As a general way to evaluate an entire set of entrainment data, a simple exponential function was used which combines the equations (20) and (24):

$$J_E = AJ_o e^{-B\frac{\sqrt{2g(H_T-H_o)}-U_o}{S_U}} \qquad (25)$$

or even simper ($A' = AJ_o$ and $B' = B/S_U$):

$$J_E = A' e^{-B'\left(\sqrt{2g(H_T-H_o)}-U_o\right)} \qquad (25a)$$

This equation allows an experimenter to find from a semi-logarithmic graph the coefficient *B'* (the slope of the curve) and from this value to find the average variance in velocity S_U, for an entire data set.

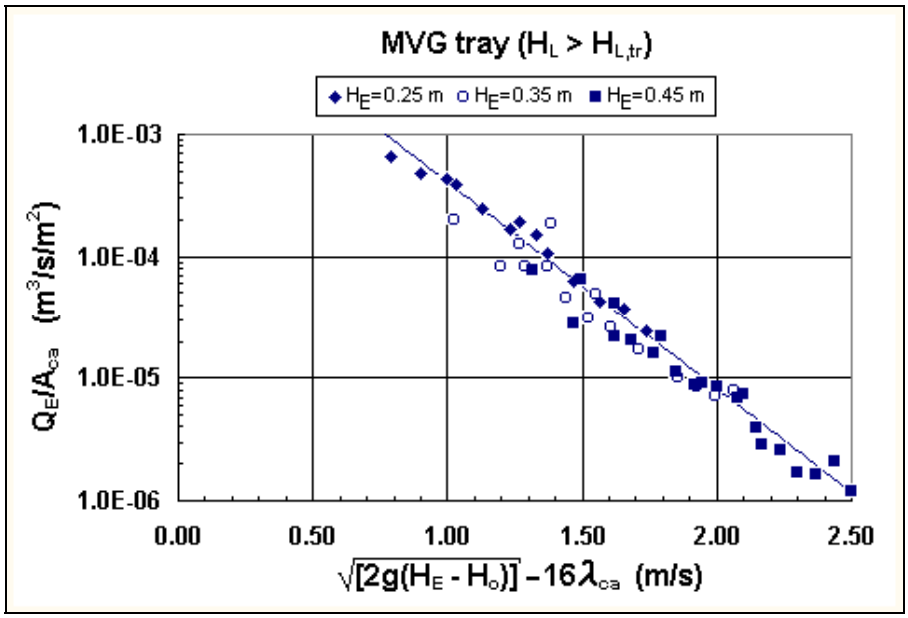

Figure 6. Entrainment rate of MVG tray at high liquid heights

The combined set of entrainment rate data for the MVG tray was correlated by the entrainment correlation as proposed (figure 6). The effect of gas flow rate on lowering the ejection plane H_o has now been included. After optimisation of the regression, the following relation summarizes the entire data set ($R^2 = 0.965$):

$$J_E = \frac{Q_E}{A_{ca}} = 0.049e^{-4.58\left(\sqrt{2g\left(H_E - 0.74H_W + \frac{142\lambda_{ca}^2}{g}\right)} - 16.2\lambda_{ca}\right)} \qquad (32)$$

Several observations arise from a comparison of equation (32) with equation (25a):

- the plane of origin H_o moves up and down as, $H_o = 0.74H_W - 142\lambda_{ca}^2/g$,
- the mean droplet projection velocity varies as $U_o = 16.2\lambda_{ca}$ m/s,
- the standard deviation in the droplet velocity distribution was derived from the B'-coefficient in the exponent (B' = –4.58) which gives a constant $S_U = 0.34$ m/s.
- the pre-exponential factor represents the initial upward liquid flux. This initial flux appears to be constant.

The Transition from Two to Three-Layers

The height of the weir at this transition is found by using the above equation (32) in combination with the value of the minimum entrainment flux in the entrainment versus weir height plot or by using its plateau value below the transition. Having obtained the position of weir $H_{W,tr}$, it is further possible to obtain the liquid height at the transition $H_{L,tr}$ from a separately obtained (and will be reported in detail in [4]) relationship between weir height and clear liquid height. By this method the results in table 5 were obtained:

Table 5. MVG tray, the transition heights

λ_{ca} (m/s)	$H_{W,tr}$ (m)	$H_{L,tr}$ (m)	$H_{o,tr}$ (m)
0.039	0.067 ± 0.018	0.034 ± 0.004	0.028 ± 0.016
0.059	0.076 ± 0.018	0.029 ± 0.004	0.006 ± 0.014
0.078	0.106 ± 0.016	0.036 ± 0.003	-0.010 ± 0.012

In a statistical sense, the values for the liquid height at transition can be considered constant at $H_{L,tr} = 0.033 \pm 0.004$ m. Accepting the above obtained relation for the position of the plane of origin of the droplets $H_o = 0.74H_W - 142\lambda_{ca}^2/g$, the position of this plane at the transition can be found, $H_{o,tr}$. Their values confirm that the bottom of the spray layer had arrived at or near the tray deck.

Entrainment, General

For all trays tested, the plots of entrainment rate versus liquid height (or weir height) showed tested *two distinct ranges* in the entrainment behaviour with a transition in between. At a low liquid height, the entrainment rate could be either increasing by an increase in liquid height or decreasing with an increasing liquid height. At a high liquid height, the entrainment rate increased monotonously for the three standard gas rates (with curves running in parallel in a logarithmic plot). In the transition range (from about 0.03 to 0.05 m), there was either *a break* in the curve or *a minimum* in the entrainment rate. The recognition of the existence of the two ranges in the entrainment behaviour was important. Especially because this pattern repeated itself on all trays tested in this study.

Having found this transition in the entrainment behaviour, the literature was consulted to find whether it had been reported before. Only, one reference could be located which described the same phenomenon, be it for trays called 'flow-guide sieve plates'. It appeared that Ye, Shi and Zhou [19] had discovered the minimum in the entrainment rate curve versus the clear liquid height at a 'critical' liquid height of $H_{L,tr} \cong 0.030..0.035$ m, in 1985 already. They noticed the similar differences in behaviour below and above the transition. Especially, that in the 'low-liquid-height' range the hole diameter had a strong effect on entrainment and that this is absent in the 'high-liquid-height' range. Two other references need to be mentioned in which a minimum in the entrainment rate has been reported as function of the liquid weir flow rate [20, 21], although a connection to the clear liquid height (and weir height) was not made.

Minimum in Entrainment Rate

Reviewing the results for the liquid height $H_{L,tr}$ and the position of the originating plane of the droplets $H_{o,tr}$, an interesting pattern can be seen. First of all, it should be reminded, that for all seven trays tested, the liquid height at this transition was found to be fairly independent of the gas flow rate (in the range tested). For five of the trays the break occurs when the bottom of the spray layer arrives at or near the tray deck. The exceptions being the two sieve trays which both have a low free area. High velocity gas jets penetrating 'deeper' into the bottom layer are thought to have contributed to a 'premature' disappearance of the intermediate layer.

Table 6. For all seven trays: the transition heights

Tray type	$H_{L,tr}$ (m)	$H_{o,tr}$ (m)
MVG	0.033 ± 0.004	at or near the tray
μVG	0.017 ± 0.004	at the tray
ST85	0.039 ± 0.004	at a fixed position (0.06 to 0.08 m)
ST27	0.053 ± 0.003	at a fixed position (0.08 to 0.09 m)
KS4	0.041 ± 0.009	at or near the tray
KS6	0.045 ± 0.006	at or near the tray
BDH375	0.035 ± 0.007	at or near the tray

The liquid height at transition $H_{L,tr}$ appears to be specific for each tray. The fixed-valve trays require the least liquid height and the low free area sieve tray with 12 mm holes (ST 27) needs the highest liquid height to change over in entrainment behaviour.

Entrainment, 'low-liquid-height' regime ($H_L < H_{L,tr}$)

The data on entrainment rate in the range below minimum (or break) have not been evaluated quantitatively, because of an in-accuracy of measurement of the liquid height which is preventing a sufficiently accurate interpretation in this range. Therefore, the ranking the results, at H_E = 0.45 m, in the following table should be seen as indicative of the entrainment behaviour of the tested trays in this regime.

Table 7. For all seven trays: entrainment at low liquid heights

		λ_{ca} = 0.039 m/s		λ_{ca} = 0.059 m/s		λ_{ca} = 0.078 m/s	
Rank	**Tray type**	**H_W = 0.00 m Q_E/A_m (m/s)**	**H_W = 0.05 m Q_E/A_m (m/s)**	**H_W = 0.00 m Q_E/A_m (m/s)**	**H_W = 0.05 m Q_E/A_m (m/s)**	**H_W = 0.00 m Q_E/A_m (m/s)**	**H_W = 0.05 m Q_E/A_m (m/s)**
6	**MVG**	0.12×10^{-5}	0.17×10^{-5}	1.90×10^{-5}	0.84×10^{-5}	9.6×10^{-5}	5.4×10^{-5}
7	**μVG**	0.17×10^{-5}	0.10×10^{-5}	0.69×10^{-5}	0.46×10^{-5}	4.1×10^{-5}	1.8×10^{-5}
2	**ST85**	0.74×10^{-5}	0.12×10^{-5}	4.1×10^{-5}	2.0×10^{-5}	4.8×10^{-4}	3.3×10^{-4}
1	**ST27**	1.30×10^{-5}	0.83×10^{-5}	11.0×10^{-5}	9.4×10^{-5}	4.1×10^{-4}	4.8×10^{-4}
(4)	**KS4**	0.27×10^{-5}	0.37×10^{-5}	7.3×10^{-5}	1.2×10^{-5}	8.7×10^{-5}	7.5×10^{-5}
(5)	**KS6**	0.48×10^{-5}	0.31×10^{-5}	1.9×10^{-5}	1.6×10^{-5}	4.5×10^{-5}	6.1×10^{-5}
3	**BDH 375**	0.81×10^{-5}	0.56×10^{-5}	2.4×10^{-5}	1.6×10^{-5}	13.0×10^{-5}	8.3×10^{-5}

The entrainment values in table 7 clearly demonstrate that *tray type is an important parameter affecting the entrainment rate,* in this range of operation. A separate study is needed to bring more clarity in the tray specific details (orifice shape, size and pitch, etc.) of importance in entrainment generation in this regime. This study may profitably make use of already existing literature on this aspect , as in [16, 21, 22].

Entrainment, 'high-liquid-height' regime ($H_L > H_{L,tr}$)

In summary, the entrainment rate in this range is most sensitive to changes in gas flow rate, entrainment collector height and weir height:

- an increase in gas rate by some 25 to 50 % increases the entrainment rate by a factor two.
- an increase in height of the collector by about 0.035 to 0.050 m halves the entrainment rate,
- an increase in weir height by about 0.035 to 0.100 m doubles the entrainment rate (this depends on tray type).

The exponential entrainment relation (equation 25) was found to be quite successful (see equation 32) in representing the observed effects. For each particular tray, the constants in the exponential relationship were found by regression of the test data. Usually, a correlation coefficient of $R^2 \geq 0.95$ could be achieved, while the entrainment flux J_E varied over a range of over 2 to almost 3 orders of magnitude. In the regressions, the effect of gas flow rate on the lowering of the ejection plane H_o was included.

Table 8. For all seven trays: entrainment at high liquid heights

	$Q_E/A_{mat} = \mathbf{A'}\text{Exp}[-\mathbf{B'}\{\sqrt{[2g(H_E - \boldsymbol{H_o})]} - \boldsymbol{U_o}\}]$				
Tray type	**A'** **(m/s)**	**B'** **(m/s)**	$\boldsymbol{H_o}$ **(m)**	$\boldsymbol{U_o}$ **(m/s)**	$\boldsymbol{R^2}$ **(–)**
MVG	0.049	4.58	$0.74H_W - 142\ \lambda_{ca}^2/g$	$16.2\lambda_{ca}$	0.965
μVG	0.008	4.13	$0.95H_W - 145\ \lambda_{ca}^2/g$	$18.3\lambda_{ca}$	0.991
ST85	0.011	4.25	$1.00H_W - 128\ \lambda_{ca}^2/g$	$18.5\lambda_{ca}$	0.959
ST27	0.006	4.20	$1.00H_W - 128\ \lambda_{ca}^2/g$	$18.5\lambda_{ca}$	0.973
KS4	0.059	4.46	$0.56H_W - 128\ \lambda_{ca}^2/g$	$15.8\lambda_{ca}$	0.957
KS6	0.042	4.34	$0.34H_W - 108\ \lambda_{ca}^2/g$	$17.6\lambda_{ca}$	0.959
BDH375	0.150	4.71	$0.54H_W - 122\ \lambda_{ca}^2/g$	$16.0\lambda_{ca}$	0.956
Overall:	**0.029**	**4.38**	$\mathbf{0.70H_W - 130\ \lambda_{ca}^2/g}$	$\mathbf{17.0\lambda_{ca}}$	**0.949**

From the regressions it was found that a *correction factor for the weir height* was needed to account properly for its variation. The results suggest that this correction may depend on the type of tray. A correction as such was expected, because of the simplicity of and the assumptions used in the derivation of the position of the drop ejection plane H_o. A possible effect of tray type was unexpected, however. By contrast, the lowering of the ejection plane by an increase in gas flow rate (via the term containing λ_{ca}^2/g) was expected. The initial droplet ejection velocity showed remarkably little variation, in spite of the different tray decks used. Its value ranged between $15.8\lambda_{ca} \leq U_o \leq 18.5\lambda_{ca}$ m/s and could be treated as a constant. Its average value being $U_o = 17.3(\pm 1.1)\lambda_{ca}$ m/s.

The standard deviation in the initial ejection velocity distribution was derived from the *B*'-coefficient in the exponential function. These values showed remarkably little variation, in spite of the differences in tray decks used. The result was that the standard deviation in ejection velocity ranged between $0.33 \leq S_U \leq 0.39$ m/s. Its average value being $S_U = 0.36 \pm 0.02$ m/s.

The pre-exponential factor (*A*') and the *B*'-parameter in the exponential function were seen to be correlated. This suggested that the individual data sets for the seven trays

actually occupied approximately the same position in parameter space. Hence, an even more general relationship was obtained which holds for all seven trays tested (R^2 = 0.949 and N = 508 data points):

$$J_E = 0.029(\pm 0.010)e^{-4.38\left(\sqrt{2g\left(H_E - 0.70H_W + \frac{130\lambda_{ca}^{\ 2}}{g}\right)} - 17\lambda_{ca}\right)} \qquad (33)$$

Earlier, it was observed that the correction factor for the weir height might vary from tray to tray. Because of this, the effect of this correction was checked and found to be of minor importance. Values in the range of 0.70 to 0.75 for this coefficient were optimal. Changing the coefficient to 0.65 reduced the optimum R^2 = 0.949 to R^2 = 0.945 and changing the coefficient to 0.80 gave R^2 = 0.945, as well. So, a rather flat optimum is observed, but a correction factor differing from a value of one is helpful. An effect of type of tray deck on the correction factor could no longer be substantiated, however.

The correlation coefficient (R^2) for the general entrainment relation is in the low range of the correlation coefficients of the individually optimized tray relations of $0.94 \leq R^2 \leq 0.99$. Hence, with hardly a loss in accuracy, this general entrainment relation represents the experimental data of all individual trays successfully, for operation in the three-layered 'high-liquid-height' regime.

It is of some value to point out, that the experiments confirm that the drop ejection plane moved with weir height and gas flow rate. It can be expected that it should move also with changes in weir loading (Q_L/L_W). It had been decided to execute the experiments with a low and constant weir load to eliminate any effect of a horizontal liquid velocity component on the two-phase behaviour in the contacting area. So, the effect of a varying weir load on entrainment could not be verified in the current experiments and has to come from the outcome of other experiments.

It is good to be aware of the *exceptional constancy* of the standard deviation in the droplet velocity distribution (derived from the *B*'-value). A small change of its value could have sensitively changed the measured entrainment rates. The other variable that is responsible for the success of the entrainment relation is the pre-exponential factor (*A*'), which can be interpreted as a constant initial flux of ejected droplets.

Checking the Transition

From a separate interpretation of the liquid height results [4], the liquid fraction in the liquid-continuous layers was found to vary inversely proportional to the gas flow rate: $\varepsilon_{L,uw}\lambda_{ca} = 0.013$ m/s.

By using this empirical result, the following equation was obtained (with dimensional constants):

$$H_{L,tr} = 0.013\frac{H_{btm}}{\lambda_{ca}} + 0.19c_h\left(1 - \varepsilon_{G,s}\right)\lambda_{ca} \qquad (34)$$

Taking the weir height ($H_{W,tr}$) at which the break in the entrainment curve occurs as a good approximation to the height of the bottom layerH_{btm}, the transition liquid height can be estimated. Also assuming $c_h(1 - \varepsilon_{G,s}) \cong 1.0$ and $H_{W,tr} \cong 0.075$ m (as a reasonable average for most trays tested). The transition liquid height at the three

standard load factors becomes $H_{L,tr} = 0.033$ m for $\lambda_{ca} = 0.038$ m/s; $H_{L,tr} = 0.028$ m for $\lambda_{ca} = 0.059$ m/s and $H_{L,tr} = 0.027$ m for $\lambda_{ca} = 0.078$ m/s.

These values compare favorably with the transition liquid height values reported from the analysis of the entrainment rate measurements, see table 6. The fact that the transition liquid height is fairly independent of the gas flow rate is also reproduced.

On the Entrainment Measurement

For comparative purposes to find an effect of different trays on entrainment rate, the measurement technique as used appears to be quit useful. It is also simple, quick to execute and able to cover a wide range of entrainment rates. The first attempt at correlating the obtained entrainment data in the small scale tray simulator was quite successful. To assess the applicability of small scale data to the operation of a large scale tray, the differences introduced by scale enlargement have to be considered. Is the entrainment rate measured on a small scale simulation tray (bounded by sidewalls) different from the rate measured above a large tray, at the same conditions. Using an entrainment collector with the same dimensions on both scales does this collector receive above a sufficiently large tray the same or more entrainment? How does this depend on the vertical position of the collector?

By some simple arguments, the principle can be shown. The vertical downward projection of the area of the entrainment collector on the top of the dispersion will be called the 'footprint'. In the small column this 'footprint' has essentially the same size as the area of the mesh pad and there is no additional area outside the 'footprint', because of the presence of the four sidewalls. On a tray of a sufficiently large diameter there are no nearby sidewalls and the area available outside the 'footprint' does contribute to the measured entrainment rate. The horizontal component of the ejection velocity of the drops can displace them sufficiently to hit the mesh pad during their flight. A detailed calculation is rather difficult because of the nature of the ejection velocity distribution function involved. An approximate way to get at a reasonable estimate of the magnitude of this 'side wall' effect is possible, however.

For a sufficiently large tray, the collected liquid flow comes from two areas, inside and outside the 'footprint'. In principle, the area outside the footprint can deliver only one half of its upward splashing drops to the mat. The other half is jumping in the opposite direction. Hence, $Q_E = f_E J_o A_{inside} + 1/2 f_E J_o A_{outside}$. So, $J_E = f_E J_o(1 + 1/2(A_{outside}/A_{mat}))$ and the entrainment correction factor becomes $(1 + 1/2(A_{outside}/A_{mat}))$ which amounts to estimating the ratio of the areas outside and inside the 'footprint'. The amount of area outside the footprint can be obtained from the horizontal distance L_{hor} travelled by the droplets before reaching the collector. This distance $L_{hor} = S_{U,\,hor} t_f$. For drops just reaching the mat at the top of their trajectories, $t_f = U_o/g$. Thus, $L_{hor} = S_{U,\,hor} U_o/g$. The average velocity of the drops reaching the mat is somewhat larger than $U_o \cong \sqrt{[2g(H_E - H_o)]}$. Thus $L_{hor} \cong S_{U,\,hor}\sqrt{[2g(H_E - H_o)]}/g$. Applying this to a square collector in a square small scale column with side wall length W, the correction factor becomes $(1 + 1/2(4L_{hor}/W))$ which can be written as:

$$\frac{J_E}{f_E J_o} = 1 + 2S_{U,hor}\frac{\sqrt{2g\left(H_E - H_o\right)}}{gW} \qquad (35)$$

For the experimental column with $W = 0.2$ m, $0.15 \le (H_E - 0.7H_W) \le 0.45$ m and $S_{U,hor} \cong S_{U,vert} = 0.36$ m/s, the correction factor is expected to vary as $(1 + 1.6\sqrt{(H_E -}$

$0.7H_W$)) which falls in the range 1.6..2.1. So, the sidewalls in a small-scale column do have a significant effect in stopping 'imaginary' drops coming from outside the 'footprint' area, that do contribute on a large scale tray. It is recommended to improve on this provisional approach and study the effects of the horizontal and vertical velocity distributions on this correction factor, in more detail. In applying the above presented general entrainment relationship obtained on a small scale simulation tray to large-scale trays or for comparing results from other studies, a suitable correction factor should be taken into account.

Comparison with FRI Data

To test the proposed maximum vapour capacity relationship (equation 28) flooding data are needed. Flooding test data for sieve trays have been published by Fractionation Research Inc. (F.R.I.). Two sieve trays of 8% and 14% hole area with holes of 12.7 mm diameter were studied. The test data were obtained in a 1.2 m diameter column with the cyclohexane/n-heptane and isobutane/n-butane test systems [23, 24]. The entrainment data for the 8% hole area sieve tray of these tests were analysed by Porter and Jenkins [20] in 1979 already. They produced a graph showing entrainment rate at constant vapour rate versus weir load (Q_L/L_W). This graph was compared to a graph (from [24]) showing the vapour rate needed to produce a specified entrainment rate versus weir load (Q_L/L_W). The graph of entrainment rate showed a *minimum in entrainment rate* in a specific range of weir loads. The other graph showed a *maximum in vapour rate,* in the same range of weir loads for which the entrainment was at a minimum. Recently, Ohe, Stupin and Yanagi [25] have re-analysed the original data and also included the entrainment results for the 14% hole area sieve tray [24].

An important observation to make from the test data is about the position of the minimum entrainment rate and the maximum in vapour rate. It is positioned at the same weir load, $Q_L/L_W \cong 1.0\times10^{-2}$ (m^3/s)/m, *for both trays* (which showed that the free hole area had no effect). The maximum load factor reached was $\lambda_{ca,max} \cong 0.12..0.13$ m/s, with cyclohexane/n-heptane at 165 kPa. The weir height and the weir length were the same on both trays: $H_W = 0.051$ m, $L_W = 0.94$ m. According to our model, the entrainment minimum and the capacity maximum are reached when the drop ejection plane has reached the bottom layer on the tray deck. For this to be the case in equation 12, the weir load term just balances the combination of the weir height and drop ejection velocity term. For the last combination the result from our tests on the small scale trays is used (see equation 33 and table 8), this leads to: $(Q_L/L_w)/(\varepsilon_{L,o}u_{L,ow}) \cong 130(\lambda_{ca}^2/g) - 0.70H_W$.

When solved for the remaining parameter and using $\varepsilon_{L,o} \cong \varepsilon_{L,uw}$ and again $\varepsilon_{L,uw}\lambda_{ca} = 0.013$ m/s, the average 'splashing drop' velocity over the weir must have been:

$$u_{L,ow} \cong (Q_L/L_w)/[\varepsilon_{L,o}(130(\lambda_{ca}^2/g) - 0.70H_W)] \cong 0.53..0.58 \text{ m/s}.$$

As expected this velocity is of the same order of magnitude of the spread in ejection velocity, $S_U \cong 0.36$ m/s, for the small scale tray tests. But, it is significantly higher which points to a better developed top ('spray') layer on a large scale tray. This is a manifestation of the same scale effect as noted by Davies and Porter [9], in 1965 already. By accepting the derived large scale value, the transition liquid height on the sieve trays can be found:

$$H_{L,tr} = \varepsilon_{L,uw}H_W + 2(Q_L/L_w)/u_{L,ow} \cong 0.040..0.043 \text{ m}.$$

These values are fully compatible with the transition liquid height values found in the small scale tests (see table 6). From this it is concluded that the transition seen in the

large scale tests is the same as seen on the small scale. Although the way in which the liquid hold up on the trays is generated is quite different. On the small scale this was done by changing the weir height and on the large scale by variation of the weir load.

The increase in entrainment rate (and consequently the drop in maximum vapour capacity) with weir load should be consistent with the model, as well. To check this equation 28 will be used. First it will be used at the transition ($Q_L/L_W \cong 1.0\times10^{-2}$ $(m^3/s)/m$) to find the missing c_{max}-parameter (unknown basically, because the entrainment rate at flood is unknown). Thereafter, the expected maximum vapour load at a 2.5-times higher weir load ($Q_L/L_W \cong 2.5\times10^{-2}$ $(m^3/s)/m$) will be estimated. The tray spacing was $H_T = 0.61$ m, assuming $S_U \cong 0.55$ m/s and $\sqrt{(1-\varepsilon_{G,df})}/12 \cong 0.074$, than at the transition $c_{max} \cong 3.2$. At the higher weir load of $Q_L/L_W \cong 2.5\times10^{-2}$ $(m^3/s)/m$, the base of the droplet layer has moved up from the tray to approximately:

$H_o \cong (2.5\times10^{-2} - 1.0\times10^{-2})/(\varepsilon_{L,o}u_{L,ow}) \cong 0.027/\varepsilon_{L,o} \cong 2.1\lambda_{ca}$

For weir loads in excess of the transition weir load, the maximum vapour capacity is:

$\lambda_{ca,max} \cong 0.074\sqrt{[2g(H_T - H_o)]} - 0.13 \cong 0.074\sqrt{[2g(0.61 - 2.1\lambda_{ca})]} - 0.13.$

This yields a drop in vapour capacity to $\lambda_{ca,max} \cong 0.085$ m/s, i.e. a reduction to about 65 to 70% of its highest value. The FRI flood tests showed a reduction also ... to about 65 to 70% of the maximum value. Indeed, the direction and magnitude of the effect can be explained.

Now, it is worthwhile to have a second look at the relation used to do the estimation and note the contributions of the two term on the right-hand side:

$\lambda_{ca,max} \cong 0.074\sqrt{[2g(H_T - H_o)]} - 0.13$ m/s.

The first of these two terms varied in the range from $0.21 < 0.074\sqrt{[2g(H_T - H_o)]} < 0.26$ m/s. Compare this with the last term. This last term represents the contribution of the high-velocity tail of the drop ejection velocity distribution, which is responsible both for the generation of the entrainment and for the dispersion height. Its influence primarily depends on the spread in the velocity distribution. i.e. the state of 'restlessness' in the dispersion. Measures that help to reduce the spread in drop ejection velocity should lead to significantly higher maximum capacity of trays. A creative tray developer might try to do this by: 1) affecting the ejection velocity distribution at the point of droplet generation, i.e. in the dispersion on the tray; 2) intercepting the drops with the highest ejection velocities just above the bulk of the dispersion before they travel up to the next tray or; 3) by a combination of the previous two approaches. Examples of attempts at developing 'high performance' trays by such means are available already. The first approach is followed by placing packing, mesh pad material or certain grid-/baffle-structures in the dispersion (for examples, see [26, 27, 28]). The second approach entails placing a droplet separator in between successive trays, examples are the 'CoFlo'™ tray (marketed by Jaeger Products Inc, Houston, USA) and the 'ConSep'™ tray (commercially available via Shell Global Solutions, Amsterdam, NL).

Tray Optimisation

A hydraulic optimal tray design can be obtained by choosing the liquid height on a tray to be just about the same as required for the dispersion to change over from a two-layered to a three-layered structure. At this transition the minimum entrainment rate is located and a maximum vapour throughput can be obtained. Also near this point, the turn down capability is at a maximum. Moreover, the tray pressure drop needed for a given separation duty is also close to a minimum (or may just have passed it).

To make a tray operate at (or near) the transition, the condition $H_{L,ca} \geq H_{L,tr}$ has to be just fulfilled.

The liquid height at the transition ($H_{L,tr}$) is a tray specific 'property', as was demonstrated before. In general: $\varepsilon_{L,uw} H_W + H_{OW} \geq H_{L,tr}$. $H_{OW} = 2(Q_L/A_{ca})(A_{ca}/L_w)/u_{L,ow}$, and so $H_{OW} = 2u_L(A_{ca}/L_w)/u_{L,ow}$.

As the flow parameter is frequently used in the tray design process, its definition is used $\varphi \cong u_L/\lambda_{ca}$ to get $u_L \cong \varphi\lambda_{ca}$. Using the (provisional empirical) relation $\varepsilon_{L,uw}\lambda_{ca} = 0.013$ m/s, as well as $u_{L,ow} = 0.6$ m/s (for large scale trays), a person 'skilled in the art of tray design' should readily see how a tray can be optimised, by writing the liquid height (with dimensional constants) as:

$$H_{L,ca} = 0.013\frac{H_W}{\lambda_{ca}} + 3.3\frac{\varphi\lambda_{ca}}{\left(L_W/A_{ca}\right)} \geq H_{L,tr} \qquad (36)$$

In general, the condition $H_{L,ca} \geq H_{L,tr}$ can be met by manipulation of the outlet weir geometry, the weir height H_W and the specific weir length L_w/A_{ca}. Note that the gas flow rate (via the loadfactor) has two counteracting effects, which make it possible to meet the condition over quite a range of gas flow rates. The current practice of using $H_W \cong 0.050$ m for most distillation tray applications is considered to be close to (although below) this minimum. Also choosing to keep applying single pass trays across the full range of flow parameters, the consequence will be that the liquid height increases during scale up and the transition liquid height will be crossed at some specific 'transition' column diameter. The 'distillation practice' of using $H_W \cong 0.050$ m leads to an approximate 'transition' value for $\varphi/(L_w/A_{ca}) \cong 0.16..0.20$. This gives a 'transition' column diameter of $D_{col} \cong (0.16..0.24)/\varphi$. For columns smaller than this 'transition' diameter, the operation would be at lower liquid heights and thus into the direction of the two-layered regime. While for larger columns, the trays would operate at higher liquid heights and so in the three-layered regime. Consequently, large diameter columns equipped with single pass trays for high pressure distillation and sour gas treating columns would be expected to operate in the 'high-liquid-height' regime.

CONCLUSIONS

A general entrainment relation for trays operating with a three-layered dispersion at higher liquid heights has been obtained. At the transition from a three-layered to a two- layered dispersion the entrainment rate is at a minimum and the maximum allowable gas rate at a maximum. For this transition a relation is proposed. An entrainment rate relation was formulated which could successfully correlate entrainment data for all seven trays tested in a small scale simulator. It is Important

that the general relation implies that an effect of tray deck type and geometry is absent, when a tray is operating in the three-layered regime. Ensuring a sufficiently high liquid height can be achieved by manipulation of the outlet weir geometry (specific weir length and the weir height).

Examination of flooding and entrainment data obtained on commercial scale test column, published by FRI, have shown that the proposed model is compatible with experimental observations on a large scale. However, a scale up effect is noted in the application of the entrainment measurement technique. A scale up effect was also noted in the development of the top ('spray') layer. Both effects need further consolidation.

The model suggests that potentially large gains in the maximum allowable vapour rate of trays should still be possible. A way to optimise the vapour capacity of existing trays has been indicated.

ACKNOWLEDGEMENTS

The support of Shell Global Solutions, SRTCA, Amsterdam, the Netherlands was indispensable. This study would not have been possible without it.

The tray deck material used during the tests was made available by Sulzer Chemtech, Tiel, the Netherlands and by Nutter Engineering, Tulsa, OK, USA.

Support by the staff of the Chemical Engineering Department of the Rijks Universiteit Groningen is gratefully acknowledged, Prof. ir. J.A. Wesselingh in particular.

SYMBOLS

Variable Parameters

A_{ca}	contacting area	m^2
A_{col}	cross section of the column	m^2
A_h	free area (of perforations) in tray floor	m^2
A_{mat}	inlet area of demister pad (entrainment collector)	m^2
$D_{B,L}$	diameter of large bubble ('void')	m
D_{col}	diameter of column	m
D_D	droplet size	m
f_h	free hole area (= A_h/A_{ca})	(---)
f_{pla}	fraction of plane of origin (at H_o) occupied by large bubbles	(---)
f_{vol}	fraction of displaced liquid volume being ejected	(---)
F	F factor, $F = U_G\sqrt{\rho_G}$ or $F = \lambda\sqrt{(\rho_L-\rho_G)}$	$m/s\sqrt{(kg/m^3)}$
F_{ca}	F-factor, based on area available for contacting	$m/s\sqrt{(kg/m^3)}$
F_h	F-factor, based on area of perforations in tray deck	$m/s\sqrt{(kg/m^3)}$
g	gravitational acceleration	m/s^2
H_{bed}	(or H_{disp}) height of two phase layer on tray	m
H_{btm}	height of bottom layer on tray deck	m
H_E	height of entrainment collector (demister pad) above tray floor	m

H_L	equivalent clear liquid height in the contacting area	m
H_L^{top}	clear liquid height in the top ('spray') layer	m
$H_{L,tr}$	clear liquid height at transition	m
H_o	height of transition from liquid-continuous to gas-continuous phase	m
H_{ow}	liquid height above the outlet weir	m
$H_{ow,ca}$	liquid height above the level of the weir, in the contacting area	m
H_T	tray spacing (distance between trays)	m
H_W	outlet weir height	m
J_E	entrainment flux, collected by demister pad at H_E	$(m^3/s)/m^2$
J_o	initial liquid flux of ejected drops at H_o	$(m^3/s)/m^2$
L_{hor}	horizontal travel distance (drop jumping distance)	m
L_W	lenght of outlet weir	m
L_W/A_{col}	specific weir lenght per unit column area	m/m^2
N	number	(---)
P( )	probability	(---)
Q_E	flow rate of collected entrainment	m^3/s
Q_G	volumetric gas flow rate	m^3/s
Q_L	volumetric liquid flow rate	m^3/s
Q_L/L_w	specific liquid weir load	$m^3/s/m$
R^2	correlation coefficient	(---)
S_U	variance (spread) in velocity distribution	m/s
t_f	time of flight of drops	s
$u_{L,ca}$	horizontal liquid flow velocity, in the contacting area	m/s
$u_{L,ow}$	horizontal liquid flow velocity, over weir	m/s
$U_{B,L}$	large bubble rise velocity	m/s
$U_{G,ca}$	superficial gas velocity, based on contacting area	m/s
$U_{G,h}$	superficial gas velcoity, based on area of perforations in tray deck	m/s
$U_{L,ca}$	liquid velocity	m/s
U_o	initial droplet projection velocity, at horizontal plane at H_o	m/s

Constant Parameters

a, b, ..	(locally specified) coefficient	(---)
A, B, ..	(locally specified) coefficient	(---)
c_h	correction factor in liquid height relation for top layer (equation (3))	(---)
c_{max}	factor in maximum gas rate equation ( )	(---)
c_{SU}	correction factor in bed height equation	(---)
f	factor	(---)
k	multiplier (as in kS_U, see equation (11))	(---)

Greek Symbols

ε_G	gas fraction in two phase layer	(---)
$\varepsilon_{G,s}$	gas fraction of small bubbles in the 'liquid'-continuous phase	(---)
ε_L	liquid fraction in two phase layer, $=H_L/H_{bed}$	(---)
$\varepsilon_{L,o}$	liquid volume fraction in the plane of origin of droplets (at H_o)	(---)
$\varepsilon_{L,ow}$	liquid volume fraction, over weir	(---)

$\varepsilon_{L,uw}$	liquid volume fraction, under weir	(---)
λ	vapour load factor, $=F/\sqrt{(\rho_L-\rho_G)}$	m/s
λ_{ca}	vapour load factor based on contacting area, $=(Q_G/A_{ca})\sqrt{[\rho_G/(\rho_L-\rho_G)]}$	m/s
λ_h	vapour load factor based on free hole area, $=(Q_G/A_h)\sqrt{[\rho_G/(\rho_L-\rho_G)]}$	m/s
φ	flow parameter, $=(Q_L/A_{col})\sqrt{\rho_L}\ /\ (Q_G/A_{col})\sqrt{\rho_G}$	(---)
ρ_G	gas density	kg/m^3
ρ_L	liquid density	kg/m^3
ω	frequency of large bubbles erupting from 'liquid' phase	(Hz)

Abbreviations/Acronyms

BDH Balanced Dimpled Half
FA Free Area
MVG Mini V-Grid
KS In Dutch: Klep schotel (= Valve Tray)
R.O. Reverse Osmosis
ST Sieve tray
VG V-Grid

REFERENCES

1. J.R. Fair, Distillation: whither, not whether, in Distillation and Absorption 1987, Brighton, *I.Chem.Engrs, Symposium Series* No. 104:A613, (1987), ISBN 0 85295 209 0.

2. F.J. Zuiderweg, in Distillation and Absorption 1987, Brighton, *I.Chem.Engrs, Symposium Series* No. 104:A589, (1987), ISBN 0 85295 209 0.

3. A.H. v. Sinderen, R.W.J. v. Zanting, J.A. Wesselingh, E.F. Wijn, "Groningen Tray Test Rig. Data Report", December 2000, (MS Word + Excel version available from E.F.W.)

4. A.H. v. Sinderen, R.W.J. v. Zanting, J.A. Wesselingh, E.F. Wijn, "Groningen Tray Test Rig. Final Report", (in preparation).

5. M.A. Jeronimo and H. Sawistowski, Characterization of dispersion in the spray regime of sieve-plate operation, Distillation 1979, *I.ChemE. Symposium Series* No. 56, (1979), pp. 2.2/41 - 2.2/56.

6. P.A.M. Hofhuis and F.J.Z. Zuiderweg, Sieve plates: dispersion density and flow regimes, *I.Chem.E., Symposium Series* No. 56, (1979), pp. 2.2/1 - 2.2/26.

7. D.L. Bennett and A.S. Kao, A mechanistic analysis of sieve tray entrainment, *A.I.Ch.E. Annual Meeting*, Chicago, Illinois, USA, (1990), paper 71a.

8. D.L. Bennett, A.S. Kao and L.W. Wong, A mechanistic analysis of sieve tray froth height and entrainment, *AIChE Journal*, 41, (1995), 9, pp. 2067-2082.

9. B.T. Davies and K.E. Porter, Some observations on Sieve Tray Froths, *Symposium on two Phase Flow*, 21-23 June 1965, University of Exeter, U.K., pp. F301-F324.

10. M.J. Ashley and G.G. Haselden, Effectiveness of vapour-liquid contacting on a sieve plate, *Trans. Inst. Chem. Engrs.*, 50, (1972), pp. 119-124.

11. D.M. Newitt, N. Dombrowski and F.H. Knelman, Liquid entrainment 1. The mechanism of drop formation from gas or vapour bubbles, *Trans. Inst. Chem. Engrs*., 32, (1954), p. 244.

12. F.H Garner, S.R.M. Ellis and J.A. Lacey, The size distribution and entrainment of droplets, *Trans. Instn. Chem. Engrs.*, 32, (1954), pp. 222-235.

13. J.A. Raper, M.S. Kearney, J.M. Burgess and C.J.D. Fell, The structure of industrial sieve tray froths, *Chem. Eng. Science,* 37, (1982), 4, pp. 501-506.

14. J. Ellenberger, Analogies in multiphase reactor hydrodynamics, *Doctoral Thesis,* University of Amsterdam, 28 november 1995.

15. J.W.A. de Swart, Scale-up of a Fischer-Tropsch slurry reactor, *Doctoral Thesis*, University of Amsterdam, 4 april 1995.

16. J. Stichlmair, Grundlagen der Dimensionierung des Gas/Fluessigkeit-Kontaktapparates Bodenkolonne, *Reprotext, Verlag Chemie*, (1978), ISBN 3-527-25811-6.

17. E.F. Wijn, Weir flow and liquid height on sieve and valve trays, *Chem. Engng. Journal*, 73 (1999), pp. 191-204.

18. R.M. Thorogood and R.E. Sacks, The measurement of fundamental distillation data with a new pilot scale apparatus to simulate a commercial cryogenic tray, Distillation and Absorption 1987, *I.ChemE. Symposium Series* No. 104, (1987), pp. B101-B112.

19. Y. Ye, J. Shi, Y. Zhou, Transition in the regime of flow and the point of inflection of the rate of entrainment on a perforated plate, *Int. Chem. Engng*., 25, (1985), 1, pp. 176-181.

20. K.E. Porter & J. D. Jenkins, Distillation 1979, 3rd International Symposium, London, *I.Chem.Engrs, Symposium Series* No. 56, (1979), ISBN 0 85295 116 7, Discussion Volume, pp. 75-121.

21. P. Puppich, R. Goedecke, Investigation of Entrainment in Tray Columns, *Chem. Eng. Technol.*, 10, (1987), pp. 224-230.

22. H.Z. Kister and J.R. Haas, Entrainment from Sieve Trays in the Froth Regime, *Ind. Eng. Chem. Res.*, 27, (1988), 12, pp. 2331-2341.

23. M. Sakata and T. Yanagi, Performance of a Commercial Scale Sieve Tray, *Distillation 1979*, *I. Chem. E. Symposium Series* No. 56, London, (1979), pp. 3.2/21-3.2/34.

24. T. Yanagi and M. Sakata, Performance of A Commercial Scale 14% Hole Area Sieve Tray, *Ind. Eng. Chem. Process Des. Dev.,* 21, (1982), pp. 712-717.

25. S. Ohe, W. Stupin and T. Yanagi, Entrainment Characteristics on Distillation Trays, *AIChE Annual Meeting*, *Distillation Honors: John Kunesh Honoree*, Reno, Nevada, November 2001.

26. D.A. Spagnolo, K.T. Chuang, Improving Sieve Tray Performance with Knitted Mesh Packing, *Ind. Eng. Chem. Process. Des. Dev.*, 23, (1984), 3, pp. 561-565.

27. G.X. Chen, K.T. Chuang, C. Chien and Y. Ye, Mass transfer and hydraulics of packed sieve trays, *Gas Separation & Purification*, 6, (1992), 4, pp. 207-213.

28. G.G. Haselden, K.S. Teo and M.J. Markwell, A cartridge tray assembly for upgrading the performance of small industrial columns, *I.Chem.E. Jubilee Symp. Series* No. 73, London, (1982), pp. D13-D22.